Arabian Journal of Chemistry (2014) xxx, xxx–xxx

King Saud University

Arabian Journal of Chemistry

www.ksu.edu.sa
www.sciencedirect.com

ORIGINAL ARTICLE

Exploitation of de-oiled jatropha waste for gold nanoparticles synthesis: A green approach

Suvardhan Kanchi [a], Gopalakrishnan Kumar [b], An-Ya Lo [a,c,*], Chuan-Ming Tseng [d], Shi-Kun Chen [a], Chiu-Yue Lin [e], Tsung-Shune Chin [a]

[a] Department of Materials Science and Engineering, Feng Chia University, Taiwan, ROC
[b] Department of Environmental Engineering, Daegu University, Republic of Korea
[c] Department of Chemical and Materials Engineering, National Chin-Yi University of Technology, Taiwan, ROC
[d] Institute of Physics, Academia Sinica, Taipei, Taiwan, ROC
[e] Green Energy Development Center, Feng Chia University, Taiwan, ROC

Received 16 October 2013; accepted 20 August 2014

KEYWORDS

De-oiled jatropha waste (DJW);
Gold nanoparticles (AuNPs);
Green synthesis;
Reduction

Abstract A novel single step green-synthesis route has been developed for the synthesis of gold nanoparticles using aqueous extract of *de-oiled jatropha waste* (*DJW*). *DJW*, a second stage waste, was adopted as a reducing agent to reduce $HAuCl_4$. Different optimal parameters such as ratio of $HAuCl_{4(aq)}/DJW_{(aq)}$, reaction temperature and pH effects were also studied to fine-tune the shape of the gold nanoparticles (AuNPs). The resultant AuNPs were characterized by UV–visible spectrometry, Transmission electron microscopy, Selected area electron diffraction, Powder X-ray diffraction and Fourier transform infrared spectroscopy. Triangle, hexagonal and spherical shaped AuNPs were obtained with the average particle size of ~14 nm. Furthermore, the AuNPs were capped and efficiently stabilized by protein molecules present in the *DJW*. In short, this novel synthesis route provides an environmental friendly and low cost option, as compared to currently available expensive chemical and/or physical methods.

1. Introduction

With the world's growing demand for energy, alternative green energy technologies were getting much attraction recently. Biodiesel is one of the major alternative fuels adopted worldwide. Undoubtedly, abundant amount of solid wastes generated accompanies biodiesel extraction. Therefore, recycle or utilization of such waste materials becomes a crucial research topic. Recently, gold nanoparticle (AuNP) synthesis has been considered as a significant area in the field of material science due to their distinctive and tunable surface plasmon resonance, which

* Corresponding author. Tel.: +886 4 23924505x7508; fax: +886 4 23926617.
E-mail address: aylo@ncut.edu.tw (A.-Y. Lo).

Peer review under responsibility of King Saud University.

ELSEVIER Production and hosting by Elsevier

http://dx.doi.org/10.1016/j.arabjc.2014.08.006
1878-5352 © 2014 Production and hosting by Elsevier B.V. on behalf of King Saud University.

plays an vital role in biomedical applications such as tissue imaging, photo-thermal therapy and drug delivery (Huang, 2006). An environmental-friendly protocol was proposed for the synthesis of AuNPs, without the usage of hazardous chemicals, to avoid adverse effects in medical applications. Subsequently, techniques such as lithography, ultrasonics, photochemical reduction and UV–irradiations have gained much attention to synthesize AuNPs (Raveendran et al., 2003). However, these techniques are expensive (Sau et al., 2001; Magnusson et al., 1999; Narayanan and Sakthivel, 2008). Fortunately, growing knowledge toward green chemistry has led the aspiration in nano-research for the synthesis of nanoparticles mediated by waste materials.

The control of composition, size, shape and dispersity is an important factor for the development of novel, facile and economically viable protocols. Among all the synthesis routes, plant-mediated and biological ways are especially suitable due to their effortlessness and eco-friendliness. For instance, plants, such as Alfalfa (Gardea-Torresdey et al., 2002, 2003), Aloe-vera (Chandran et al., 2006), Cinnamomum camphora (Huang et al., 2007) (see Table 2) have been well studied as prospective reductants for the synthesis of AuNPs.

Even though many economical reductants have been reported for the green synthesis of AuNPs, *de-oiled jatropha waste* (*DJW*) as an economical and eco-friendly material, has not yet been studied and entered in the scientific literature. Utilization of this second stage, *DJW,* as a reductant for the bio-synthesis of AuNPs is a win–win strategy because it not only converts the waste into a useful material but also prevents on-site burning of the waste and saves on disposal costs.

Here is a report on a "greener" synthesis method for the preparation of AuNPs using *DJW*. The term "greener" is used since naturally renewable energy waste material, 1 a second stage waste is used not only as reducing but also as protecting agent. Last but not the least, the proposed synthesis route is carried out at a negligible energy input.

2. Experimental

2.1. Procurement of *DJW* raw material

Lin et al. has been working on the production of bio-hydrogen from *de-oiled jatropha waste*, (Kumar et al., 2012; Kumar and Lin, 2013), which is obtained from a biodiesel company (Hua Neng Pvt. Ltd, Central Taiwan) after the extraction of vegetable oil from the abovementioned biomass (Aromal et al., 2012). *DJW;* a second stage waste material was used in this study. The exploration of this waste for energy (hydrogen) production has been reported in the literature (Kumar et al., 2012; Kumar and Lin, 2013). In this study, *DJW* procured from the Green Energy Development Centre, Feng Chia University, Taiwan was used for the synthesis of AuNPs as shown in Scheme 1, where detailed qualitative and quantitative composition was illustrated in earlier reports (Kumar et al., 2012; Kumar and Lin, 2013) as depicted in Table 1. 20 g of *DJW* was diluted in 70 mL of water and heated to 45 °C for 30 min and the extract was collected, filtered and ready for use.

2.2. Synthesis of AuNPs

In the present investigation, a facile, cost effective and single step green synthesis of AuNPs with $DJW_{(aq)}$, at room temperature was explored. First, 50 mg of $HAuCl_4 \bullet 3H_2O$ (Chloroauric acid; Sigma–Aldrich Chemicals) was dissolved in 120 mL of doubly distilled deionized water. For each experiments, 25 mL of $HAuCl_{4(aq)}$ was added into a beaker of 100 mL and stirred for 10 min prior to the addition of $DJW_{(aq)}$. After one hour, the color of mixture solution became orange from pale yellow, which represents the reduction of Au(III) to Au(0), indicating the formation of AuNPs. The experiment was repeated with a series of different conditions. By which, effects of $DJW_{(aq)}$ quantity (7–20 mL), which is later expressed in terms of the ratio $HAuCl_{4(aq)}/DJW_{(aq)}$, reaction temperature [RT (30–60 °C)], and pH value (3.0–6.0), were investigated.

2.3. Characterization methods

The specimens of AuNPs were ultrasonically agitated in acetone to disperse and then dried on a copper grid prior to the high-resolution transmission electron microscopy (HR-TEM) and selected area electron diffraction (SAED) examination (JEOL JEM-2100F) operated at 200 keV. The UV–visible spectra were recorded on a V-550 UV–visible spectrophotometer with samples in quartz cuvette in the range of 200–800 nm. Powder X-ray diffraction (XRD) measurements were carried out (Philips X'Pert PRO) using CuKα (0.154 nm) radiation (45 kV, 40 mA), operating at 40 kV and 40 mA. The FT-IR spectra were also recorded using a Perkin–Elmer FT-IR spectrophotometer.

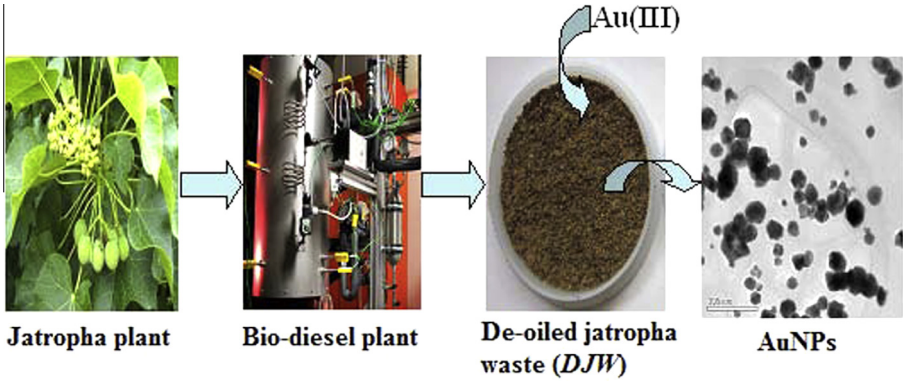

Scheme 1 Schematic drawing of green synthesis flow chart.

Table 1 Characteristics of *DJW*.

Parameters	Values
pH	6.8 ± 0.1
TCOD (g/g TS)[a]	17.1 ± 0.2
Total carbohydrate (g/g TS)	0.72 ± 0.02
Ash (w/w) (g/g TS)[b,c]	0.09 ± 0.01
Moisture (w/w)[b,c]%	6.78 ± 0.04
TKN (g/L)	8.56 ± 0.15
Total solids (%W/W)	92.6 ± 1.2
Volatile solids (%W/W)	85.4 ± 1.0
Cellulose (%)	14.1 ± 0.8
Hemicellulose (%)	28.2 ± 1.3

[a] Total chemical oxygen demand.
[b,c] Based on 10 g fresh weight (Kumar et al., 2012; Kumar and Lin, 2013).

3. Results and discussion

3.1. Optimization of experimental parameters

Considering the effect of the increment of $DJW_{(aq)}$, specimens G-7, G-10, G-15, and G-20 produced under $HAuCl_{4(aq)}/DJW_{(aq)}$ ratios of 25/7, 25/10, 25/15, and 25/20 respectively were analyzed by TEM. Fig. 1a shows the TEM image of specimen G-7. Fig. 1b–d show the TEM images of different $HAuCl_{4(aq)}/DJW_{(aq)}$ ratios of specimens G-10, G-15, and G-20, and their corresponding lattice/SAED images (insets). These images show that the size of AuNPs is strongly dependent on the $HAuCl_{4(aq)}/DJW_{(aq)}$ ratio. As the ratio decreases from 25/7 to 25/20, the average diameter of AuNPs decreases obviously from ca. 50 nm to ca. 15 nm. Similar trend was shown in SAED images as well.

Comparing with G-20, specimens T-40C, T-50C, and T-60C were prepared at 40 °C, 50 °C, and 60 °C, respectively. Fig. 2a–c show the TEM/lattice/SAED images of specimens T-40C, T-50C, and T-60C. It depicts the effect of various reaction temperatures. In general, AuNP size increases with the increase of reaction temperature. AuNP size of about 50–100 nm can be found in T-40C and T-50C and 200 nm in T-60C. Some smaller AuNPs can be seen, for example, in T-60C (ca. 10–25 nm, shown in Fig. 2c). This fact indicates that uniform AuNPs are preferred at lower reaction temperatures. Besides, reaction temperature dominates the shape of Au products as well. As shown in Fig. 2a, increasing the temperature from RT to 40 °C, some spherical nanoparticles are replaced by triangle, and hexagonal ones. The similar phenomenon can also be found in T-50C (see Fig. 2b). This is attributed to the fact that thermal energy promotes the reduction reaction

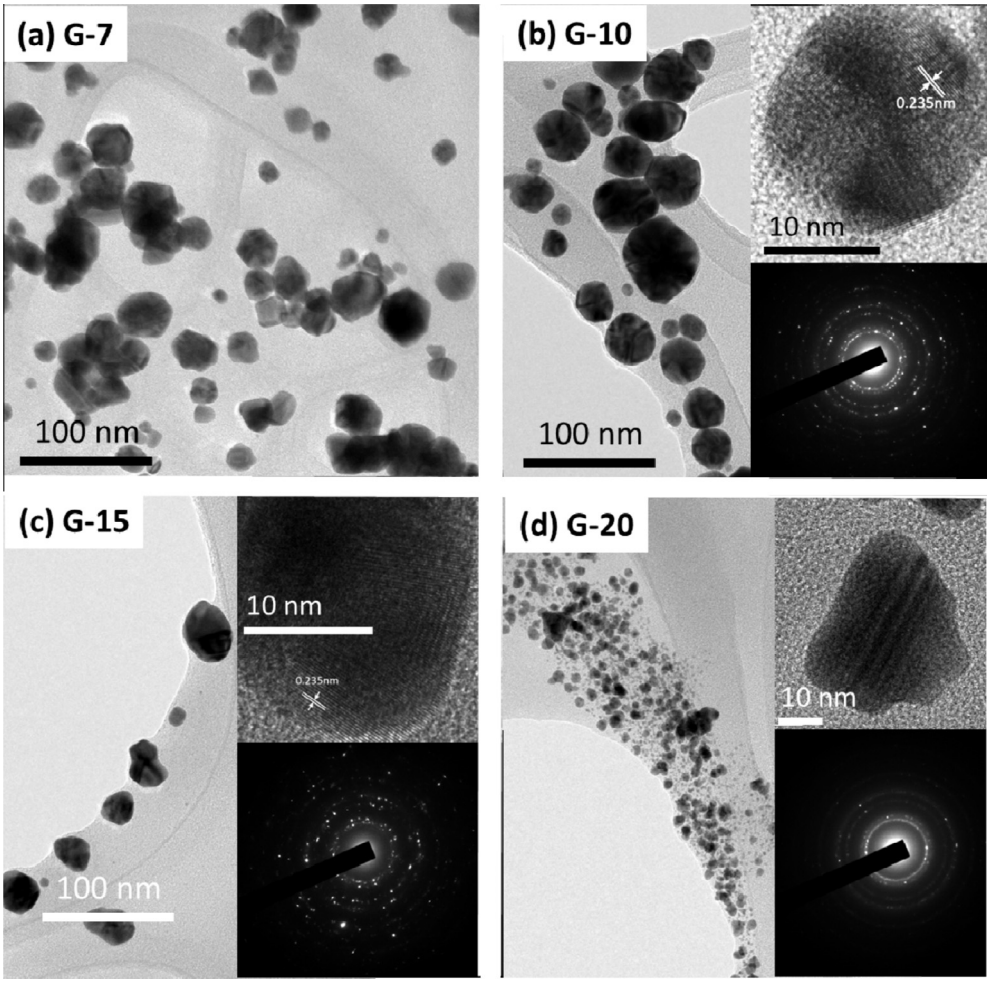

Fig. 1 TEM, and corresponding lattice and SAED images of specimen (a) G-7, (b) G-10, (c) G-15, and (d) G-20.

Table 2 Waste materials used as a reductant for Au/AgNPs preparation in the literature.

Material (Reductant)	Shapes of NPs	Nanoparticles	Cost factor		Size (nm)	Citations
			Economical	Highly economical		
Acanthella elongata	Spherical	Au	✓		~15	Inbakandan et al., 2010
Sugar beet pulp	Triangular, spherical, hexagonal, nano rods, polygonal	Au	✓		~20	Castro et al., 2010
Pear fruit extract	Triangular, hexagonal	Au	✓		~20	Ghodake et al., 2010
Cinnamon zeylanicum	Spherical	Au, Ag	✓		~20	Dwivedi and Gopal 2010
Chenopodium album leaf extract	Spherical	Au, Ag	✓		10–30	Kumar et al., 2011
Zingiber officinale	Spherical	Au	✓		5–15	Khalil et al., 2012
Olive leaf extract	Triangle, hexagonal, spherical	Au			50–100	Dubey et al., 2010
Coriander leaf extract	Triangle, hexagonal, nano rods	Au, Ag		XX	6.75–57.91	Kaviya et al., 2012
Tansy fruit	Triangle, hexagonal, spherical	Au, Ag	✓		50	Ganesh Kumar et al., 2011
Crossandra infundibuliformis	Flakes	Ag	✓		~38	Aromal et al., 2012
Cassia auriculata	Triangle, hexagonal, spherical	Ag	✓		15–25	Philip 2010
Macrotyloma uniflorum	Spherical	Au	✓		14–17	Mohan Kumar et al., 2012
Hibiscus rosa-sinensis	Triangle, hexagonal, spherical	Au, Ag		XX	~14	Bankar et al., 2010
Terminalia chebula	Triangle, hexagonal, spherical	Au	✓		6–60	Bar et al., 2009
Banana peel extract	Nano wire	Au		XX	50–60	Cruz et al., 2010
Jatropha curcas	Spherical	Ag	✓		15–50	Ghoreishi et al., 2011
Lippia citriodora	Spherical	Ag	✓		15–30	Vijayakumar et al., 2011
Rosa damascena	Spherical	Ag, Au	✓		16–18	Mukunthan et al., 2011
Catharanthus roseus	Spherical	Ag	✓		48–67	Kora et al., 2010
Crocus sativus	Spherical, triangle	Au	✓		~15	Sathishkumar et al., 2009
Cochlospermum gossypium	Spherical	Ag	✓		~3	Kumar et al., 2012
Terminalia arjuna	Spherical	Au	✓		20–50	Gopinath et al., 2013
Trigonella foenum-graecum	Hexagonal, spherical	Au	✓		15–25	Aswathy Aromal and Philip, 2012
Abelmoschus esculentus	Spherical	Au	✓		45–75	Chidambaram et al.,2013
Morinda citrifolia L.	Triangle, hexagonal, spherical	Au	✓		12.17–38.26	Suman et al., 2014
Palm oil mill effluent (POME)	Spherical	Au		XXA	18.75 ± 5.96	Pei Pei Gan et al., 2012
Tamarind leaf extract	Triangle	Au	✓		20–40	Ankamwar et al., 2005a,2005b
Emblica officinalis	Triangle, hexagonal, spherical	Au, Ag	✓		10–25	Ankamwar et al., 2005a,2005b
Lemongrass plant	Triangle	Au	✓		-	Shankar et al., 2004a,2004b
Azadirachta indica	Triangle, hexagonal, spherical	Au, Ag	✓		5–35	Shankar et al., 2004a,2004b
Geranium leaf extract	Pentagon, triangle, nanorods	Au	✓		12 ± 3	Franco-Romano et al., 2014
Solanum nigrum leaf extract	Spherical	Au	✓		32 ± 6 nm	Muthuvel et al., 2014
De-oiled jatropha waste(DJW)	Triangle, hexagonal, nanorods, spherical, cube	Au		XXA	~14	Present work

✓ = waste is economical and used as it is from the plant, XX = waste is highly economical, XXA = waste is obtained by-products and highly economical.

Please cite this article in press as: Kanchi, S. et al., Exploitation of de-oiled jatropha waste for gold nanoparticles synthesis: A green approach. Arabian Journal of Chemistry (2014), http://dx.doi.org/10.1016/j.arabjc.2014.08.006

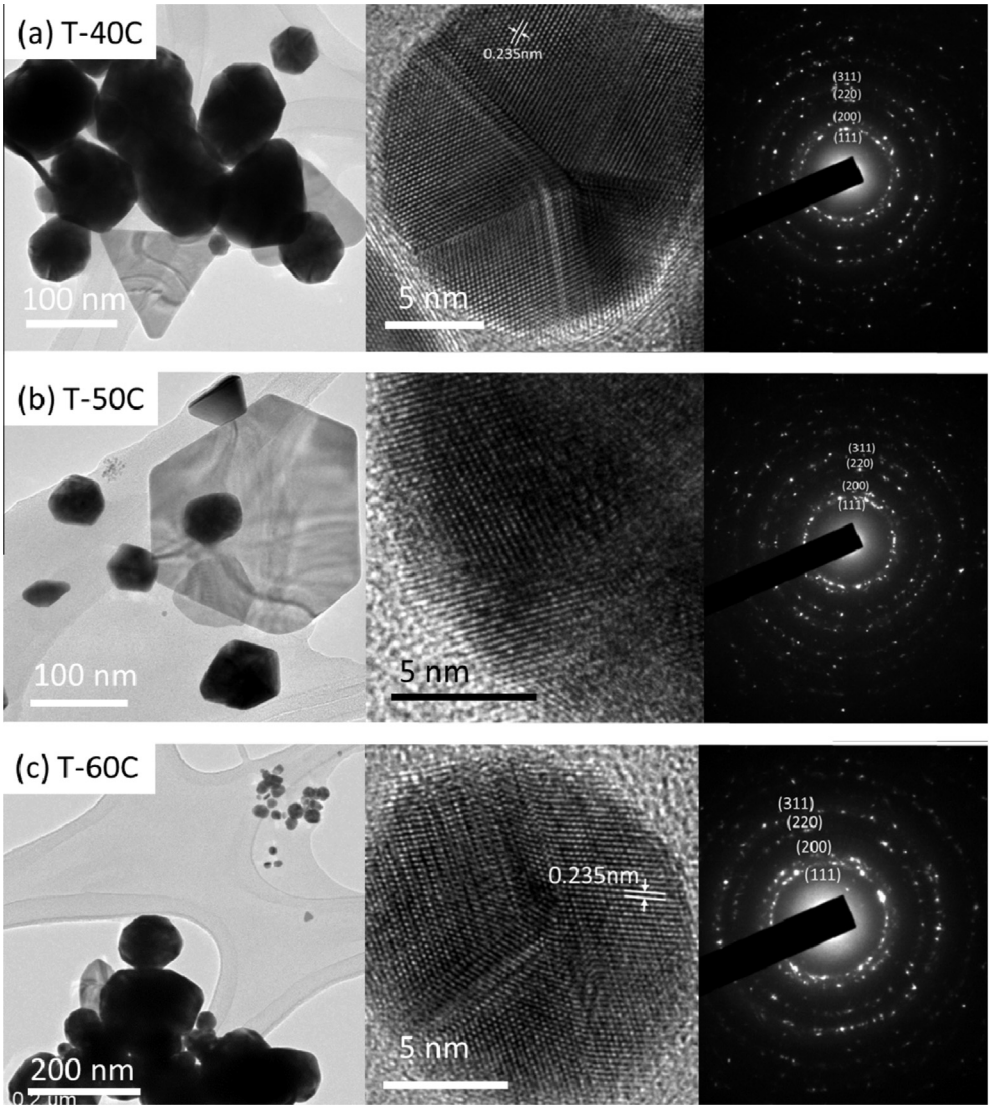

Fig. 2 TEM, and corresponding lattice and SAED images of specimen (a) T-40C, (b) T-50C and (c) T-60C.

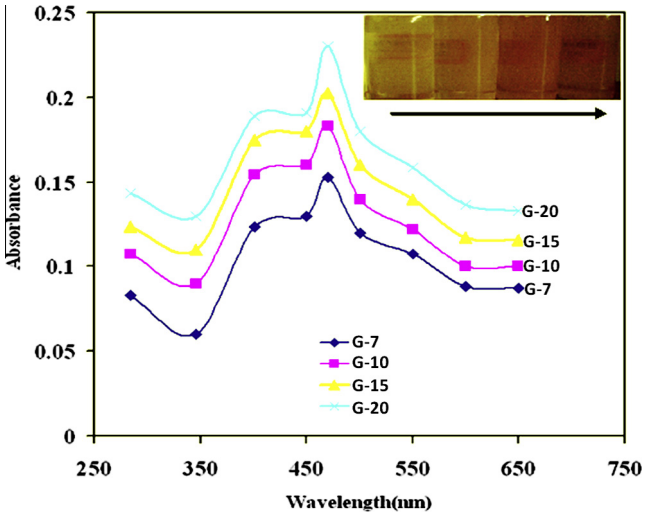

Fig. 3 UV–visible spectrum of G-7, G-10, G-15 and G-20.

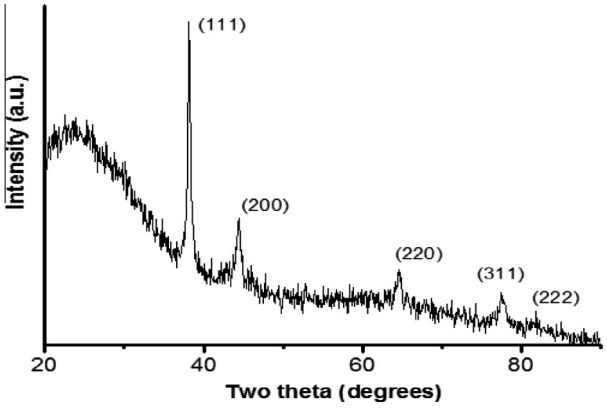

Fig. 4 X-ray powder diffraction patterns of specimen G-20.

and enhances the degree of crystallization, which is related to the maximization effect on growth anisotropy of AuNPs by the protein (Gardea-Torresdey et al., 2000; Unsworth et al.,

2005; Xie et al., 2009), being contained in the *DJW*, at around 50 °C. This inference can be supported by the comparison among lattice images of G-20, T-40C, T-50C, and T-60C, as insets in Fig. 1d and Fig. 2a–c respectively. The lattice fringes are much more manifest than that of G-20. Nevertheless, further increase of reaction temperature to 60 °C (see Fig. 2c) can only increase the particle size without abundant amount of triangle or hexagonal shaped particles. In fact, the probabilities of finding triangle or hexagonal shaped particles decrease. This is due to the fast growth rate which veils the growth anisotropy. Other than that, a minor enhancement of pH can also speed up the reduction reaction in 10 min. In short, the reaction is always fast and the colloids can usually be obtained within a few minutes, which implies the *DJW* adopted here possesses strong reducing nature in our current system [Au(III) to Au(0)].

3.2. Studies of HR-TEM, UV–visible, XRD and FTIR spectra

Interestingly, lattice images obtained by HR-TEM were adopted to check the crystallization. In general, all the lattice fringes depict a spacing of 0.235 nm which corresponds to the spacing between (1 1 1) plane of fcc Au (Aromal et al., 2012). The inter-planar distance of the Au (1 1 1) plane is in good agreement with the (1 1 1) *d*-spacing of bulk Au (0.2355 nm). Typically, spotty patterns (Figs. 1 and 2) from inner to outer corresponding to the (1 1 1), (2 0 0), (2 2 0) and (3 1 1) planes are proof that the AuNPs obtained are highly crystalline and fcc in nature.

In this study, UV–visible spectrum was adopted preliminarily to confirm the formation of AuNPs during the reduction reactions. Fig. 3 shows the UV–visible spectra of Au colloids (samples G-7, G-10, G-15, and G-20) where the inset picture shows the color of corresponding colloids changes from yellow (G-7) to pale orange (G-20). According to the spectra, surface plasmon resonance peak (520 nm) is broadened especially for G-7. As the quantity of *DJW* increases to 20 mL, the surface plasmon peak becomes slightly narrow and sharp and the color of its solution becomes pale orange. Both evidences indicate that more spherical shaped AuNPs are formed in G-20 than it is in G-15, G-10, and G-7.

Fig. 4 represents the XRD spectrum of G-20 AuNPs with the diffraction peaks at 38.1°, 44.5°, and 64.8° corresponding to (1 1 1), (2 0 0), and (2 2 0) facets of the face centered cubic crystal structure. The peak (1 1 1) plane is more intense than (2 0 0), and (2 2 1), which coincide with the aforementioned SAED results. Therefore, the (1 1 1) peak of the AuNPs is adopted to calculate the particle size by Scherrer equation. The calculation result shows an average size of ca. 14 nm for specimen G-20, is in good agreement with the statistic results made from TEM measurements (see Fig. 5).

The ingredients of *DJW* are complex, including carbohydrates, cellulose, hemicellulose, lignin and proteins (Kumar et al., 2012; Kumar and Lin, 2013). FT-IR was employed to figure out the promising biomolecules accountable for capping and competent stabilization of obtained AuNPs using *DJW*. The FTIR spectra of reduced AuNPs (G-20) and pure *DJW* are shown in Fig. 6. The broad peak at 1061 cm^{-1} corresponds to C–O stretching and the sharp peak at 1149 cm^{-1} can be attributed to C–O–C symmetric stretching and C–O–H bending vibrations of proteins present in *DJW*. Peaks around

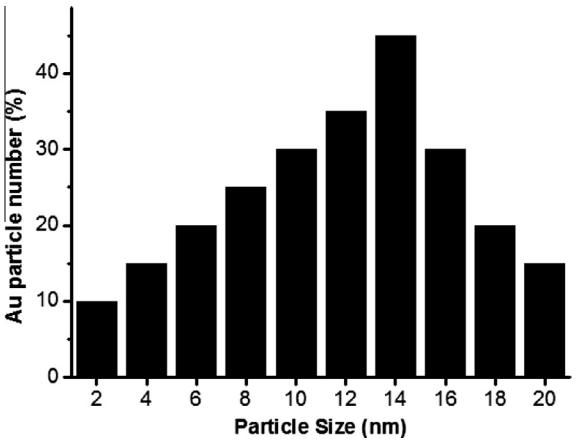

Fig. 5 Au particle size distributions of specimen G-20.

1342 cm^{-1} and 1647 cm^{-1} correspond to amide I and II bands of proteins in *DJW* (Aromal et al., 2012; Kumar et al., 2012; Kumar and Lin, 2013; Gardea-Torresdey et al., 2000; Unsworth et al., 2005; Xie et al., 2009). Free amine group or carboxylate ion of amino acids present in proteins helps to bind AuNPs strongly to avoid aggregation, (Kumar et al., 2012; Gardea-Torresdey et al., 2000; Unsworth et al., 2005; Xie et al., 2009) and as a result it controls the size and shape of nanoparticles. In addition, the presence of C═O stretching peak and –COOH groups in *DJW* is involved in the binding of AuNPs. Hence, the peaks around 1640 and 1055 cm^{-1} in the FT-IR spectra demonstrate the possibility of the binding of the free amine group of proteins to the AuNPs formed. The results of energy dispersive X-ray (EDX; shown in Fig. 7) and XRD (see Fig. 4) spectra strongly suggest the reduction of Au(III) to Au(0). In the presence of *DJW* material, Au atoms are reduced forming $AuCl_4^-$ which forms complexing agents with *DJW*. These complexing agents generate active sites on Au clusters thereby leading the formation of AuNPs of varied morphologies as shown in Scheme 2.

3.3. Evaluation of DJW with literature reported waste materials

Table 2 shows the comparison of *DJW* as a reducing agent for the synthesis of AuNPs in relation to other relevant literature

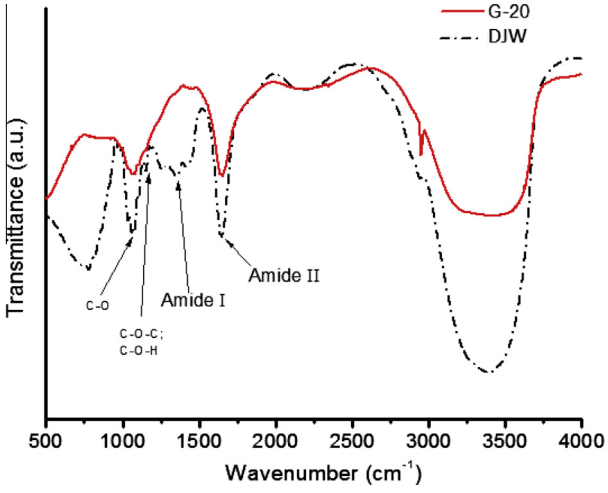

Fig. 6 FT-IR spectrum of $DJW_{(aq)}$ of specimen G-20.

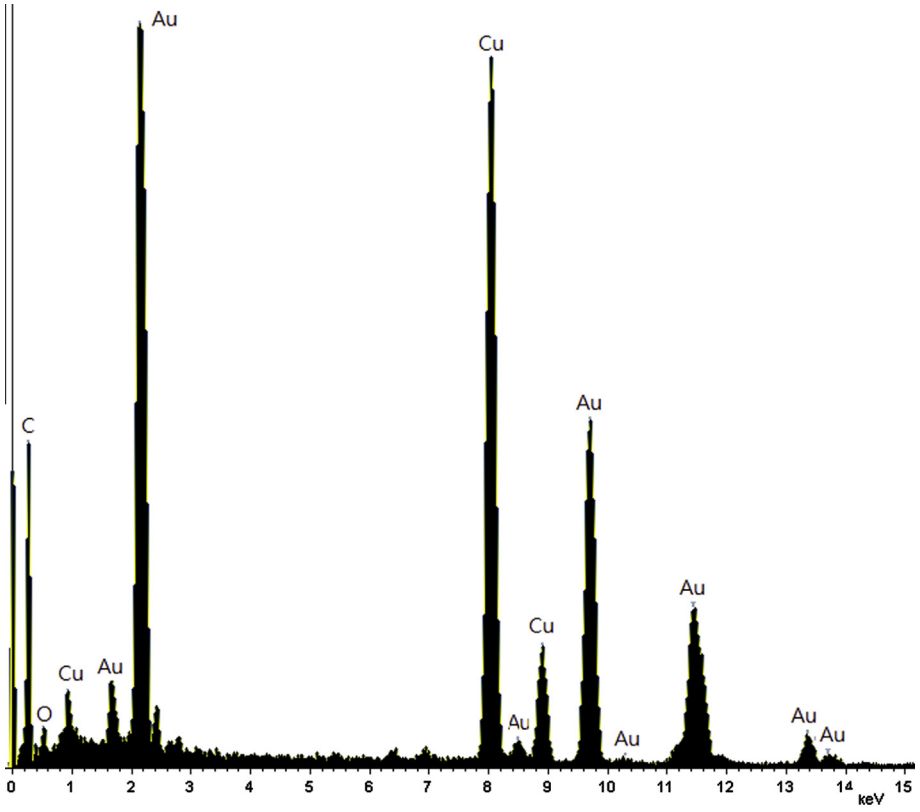

Fig. 7 Energy dispersive X-ray (EDX) of specimen G-20.

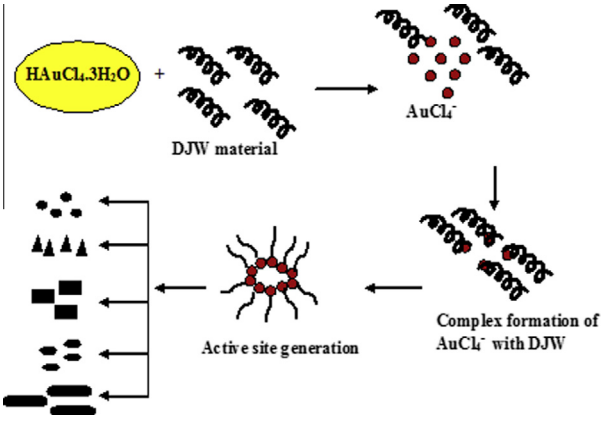

Scheme 2 Schematic of proposed mechanism of $AuCl_4^-$ reduction and AuNPs formation.

studies. The AuNPs obtained in this study are smaller (~14 nm) than those reported in the literature except nanoparticles prepared using Cochlospermum gossypium (Kora et al., 2010). Even though Cochlospermum gossypium is an economical waste material for the reduction of Au(III) to Au(0), *DJW* is highly economical and it is the by-product of renewable waste material (second stage waste). *DJW* acts as a spontaneous reducing agent (~60 min), with uniformly shaped and sized AuNPs than the already reported waste materials (Chidambaram et al.,2013; Kumar et al., 2011; Bar et al., 2009). This suggests that *DJW* could easily reduce Au(III) to form nanoparticles as mentioned in this work (see Figs. 1 and 2). In addition, the results revealed that the *DJW* could be considered as a promising material for the green synthesis of AuNPs, even when compared with reported waste materials in the literature. Furthermore, recent expansion of the bio-energy sector, *DJW* can easily be obtained without any problems at very low cost or even for free. All these indicate that *DJW* is a type of novel, highly economical, eco-friendly and cost effective reducing agent for the preparation of AuNPs.

4. Concluding remarks

In this report, a novel green synthesis route has been investigated for the preparation of AuNPs. The proposed method possesses advantages and properties over reported methods owing to the following. First of all, *DJW*, a second stage waste is a highly economical reducing agent for the conversion of Au(III) to Au(0). Second, the resultant AuNPs are formed readily at room temperature and are multi-shaped with an average particle size of ~14 nm. Besides, the proposed method is facile, rapid and cost effective and it has wide applications in commercial sectors. Due to the aforementioned properties, this method is best fit for industrial scaling of AuNPs. Finally, this study provides potential synthesis route in the field of materials science, nano-technology and green chemistry.

Acknowledgment

The authors gratefully acknowledge the financial supports by the Taiwan's National Science Council (NSC-99-2221-E-035-017-MY3, NSC-100-2811-E035-002), the Taiwan's Bureau of

Energy (grant no. 99-D0204-3) and the Feng Chia University (FCU-10G27101) to carry out this research. Technical support from the NanoCore, the Core Facilities for Nanoscience and Nanotechnology at Academia Sinica in Taiwan, is acknowledged as well.

References

Ankamwar, B., Chaudhary, M., Sastry, M., 2005a. Gold nanotriangles biologically synthesized using Tamarind leaf extract and potential application in vapor sensing. Syn. React. Inorg. Met.-Org. Nano-Met. Chem. 35, 19–26.

Ankamwar, B., Damle, C., Ahmad, A., Sastry, M., 2005b. Biosynthesis of gold and silver nanoparticles using Emblica officinalis fruit extract, their phase transfer and transmetallation in an organic solution. J. Nanosci. Nanotechnol. 5, 1665–1671.

Aromal, S.A., Vidhu, V.K., Philip, D., 2012. Green synthesis of well-dispersed gold nanoparticles using Macrotyloma uniflorum. Spectrochim. Acta Part A 85, 99–104.

Aswathy Aromal, S., Philip, Daizy., 2012. Green synthesis of gold nanoparticles using Trigonella foenum-graecum and its size-dependent catalytic activity. Spectrochim. Acta Part A 97, 1–5.

Bankar, A., Joshi, B., Ravi Kumar, A., Zinjarde, S., 2010. Banana peel extract mediated synthesis of gold nanoparticles. Colloids Surf. B Biointerfaces 80, 45–50.

Bar, H., Bhui, D.K., Sahoo, G.P., Sarkar, P., Pyne, S., Misra, A., 2009. Green synthesis of silver nanoparticles using seed extract of Jatropha curcas. Colloids Surf. A Biointerfaces 348, 212–216.

Castro, L., Blázquez, M.L., González, F., Muñoz, J.A., Ballester, A., 2010. Extracellular biosynthesis of gold nanoparticles using sugar beet pulp. Chem. Eng. J. 164, 92–97.

Chandran, S.P., Chaudhary, M., Pasricha, R., Ahmad, A., Sastry, M., 2006. Synthesis of gold nanotriangles and silver nanoparticles using Aloevera plant extract. Biotechnol. Prog. 22, 577–583.

Chidambaram, Jayaseelan., Rajendiran, Ramkumar., Abdul, Rahuman., Pachiappan, Perumal., 2013. Green synthesis of gold nanoparticles using seed aqueous extract of Abelmoschus esculentus and its antifungal activity. Ind. Crops Prod. 45, 423–429.

Cruz, D., Falé, P.L., Mourato, A., Vaz, P.D., Luisa Serralheiro, M., Lino, A.R.L., 2010. Preparation and physicochemical characterization of Ag nanoparticles biosynthesized by Lippia citriodora (Lemon Verbena). Colloids Surf B 81, 67–73.

Dubey, S.P., Lahtinen, M., Sillanpää, M., 2010. Tansy fruit mediated greener synthesis of silver and gold nanoparticles. Process. Biochem. 45, 1065–1071.

Dwivedi, A.D., Gopal, K., 2010. Biosynthesis of silver and gold nanoparticles using Chenopodium album leaf extract. Colloids Surf A 369, 27–33.

Franco-Romano, M., Gil, M.L.A., Palacios-Santander, J.M., Delgado-Jaén, J.J., Naranjo-Rodríguez, I., Hidalgo-Hidalgo de Cisneros, J.L., Cubillana-Aguilera, L.M., 2014. Sonosynthesis of gold nanoparticles from a Geranium leaf extract. Ultrason. Sonochem. 21, 1570–1577.

Ganesh Kumar, V., Dinesh Gokavarapu, S., Rajeswari, A., Stalin Dhas, T., Karthick, V., Kapadia, Z., Shrestha, T., Barathy, I.A., Roy, A., Sinha, S., 2011. Facile green synthesis of gold nanoparticles using leaf extract of antidiabetic potent Cassia auriculata. Colloids Surf. B Biointerfaces 87, 159–163.

Gardea-Torresdey, J.L., Gomez, E., Peralta-Videa, J.R., Parsons, J.G., Troiani, H., Jose-Yacaman, M., 2003. Alfalfa Sprouts: a natural source for the synthesis of silver nanoparticles. Langmuir 19, 1357–1361.

Gardea-Torresdey, J.L., Parsons, J.G., Gomez, E., Peralta-Videa, J., Troiani, H.E., Santiago, P., Yacaman, M.J., 2002. Formation and growth of Au nanoparticles inside live Alfalfa plants. Nano Lett. 2, 397–401.

Gardea-Torresdey, J.L., Tiemann, K.J., Gamez, G., Dokken, K., Cano-Aguilera, I., Furenlid, L.R., Renner, M.W., 2000. Reduction and accumulation of Gold(III) by Medicago sativa Alfalfa biomass: X-ray absorption spectroscopy, pH, and temperature dependence. Environ. Sci. Technol. 34, 4392–4396.

Ghoreishi, S.M., Behpour, M., Khayatkashani, M., 2011. Green synthesis of silver and gold nanoparticles using Rosa damascena and its primary application in electrochemistry. Physica E 44, 97–104.

Ghodake, G.S., Deshpande, N.G., Lee, Y.P., Jin, E.S., 2010. Pear fruit extract-assisted room-temperature biosynthesis of gold nanoplates. Colloids Surf. B Biointerfaces 75, 584–589.

Gopinath, K., Venkatesh, K.S., Ilangovan, R., Sankaranarayanan, K., Arumugam, A., 2013. Green synthesis of gold nanoparticles from leaf extract of Terminalia arjuna, for the enhanced mitotic cell division and pollen germination activity. Ind. Crops Prod. 50, 737–742.

Huang, S.H., 2006. Gold nanoparticle-based immunochromatographic test for identification of Staphylococcus aureus from clinical specimens. Clin. Chim. Acta 373, 139–143.

Huang, J., Li, Q., Sun, D., Lu, Y., Su, Y., Yang, X., Wang, H., Wang, Y., Shao, W., He, N., Hong, J., Chen, C., 2007. Biosynthesis of silver and gold nanoparticles by novel sundried Cinnamomum camphora leaf. Nanotechnology 18, 105104–105114.

Inbakandan, D., Venkatesan, R., Ajmal Khan, S., 2010. Biosynthesis of gold nanoparticles utilizing marine sponge Acanthella elongata (Dendy, 1905). Colloids Surf. B Biointerfaces 81, 634–639.

Kaviya, S., Santhanalakshmi, J., Viswanathan, B., 2012. Biosynthesis of silver nano-flakes by Crossandra infundibuliformis leaf extract. Mater. Lett. 67, 64–66.

Khalil, M.M.H., Ismail, E.H., El-Magdoub, F., 2012. Biosynthesis of Au nanoparticles using Olive leaf extract: 1st nano updates. Arabian J. Chem. 5, 431–437.

Kora, A.J., Sashidhar, R.B., Arunachalam, J., 2010. Gum kondagogu (Cochlospermum gossypium): a template for the green synthesis and stabilization of silver nanoparticles with antibacterial application. Carbohydr. Polym. 82, 670–679.

Kumar, G., Lay, C.H., Chu, C.Y., Wu, J.H., Lee, S.H., Lin, C.Y., 2012. Seed inocula for biohydrogen production from biodiesel solid residues. Int. J. Hydrogen Energy 37, 15489–15495.

Kumar, G., Lin, C.Y., 2013. Bioconversion of *de-oiled jatropha waste* to hydrogen and methane: influence of substrate concentration, temperature and pH. Int. J. Hydrogen Energy 38, 63–72.

Kumar, K.P., Paul, W., Sharma, C.P., 2011. Green synthesis of gold nanoparticles with Zingiber officinale extract: characterization and blood compatibility. Process. Biochem. 46, 2007–2013.

Magnusson, M.H., Deppert, K., Malm, J.O., Bovin, J.O., Samuelson, L., 1999. Size-selected gold nanoparticles by aerosol technology. Nanostruct. Mater. 12, 45–48.

Mohan Kumar, K., Mandal, B.K., Sinha, M., Krishnakumar, V., 2012. Terminalia chebula mediated green and rapid synthesis of gold nanoparticles. Spectrochim. Acta Part A 86, 490–494.

Mukunthan, K.S., Elumalai, E.E., Patel, T.N., Murty, V.R., 2011. Catharanthus roseus: a natural source for the synthesis of silver nanoparticles. Asian Pac. J. Trop. Biomed. 1, 270–274.

Muthuvel, A., Adavallan, K., Balamurugan, K., Krishnakumar, N., 2014. Biosynthesis of gold nanoparticles using Solanum nigrum leaf extract and screening their free radical scavenging and antibacterial properties. Biomed. Prev. Nutr. 4, 325–332.

Narayanan, K.B., Sakthivel, N., 2008. Coriander leaf mediated biosynthesis of gold nanoparticles. Mater. Lett. 62, 4588–4590.

Gan, Pei.Pei., Ng, Shi.Han., Huang, Yan., Li, Sam.Fong.Yau., 2012. Green synthesis of gold nanoparticles using palm oil mill effluent (POME): a low-cost and eco-friendly viable approach. Bioresour. Technol. 113, 132–135.

Philip, D., 2010. Green synthesis of gold and silver nanoparticles using Hibiscus rosa-sinensis. Physica E 42, 1417–1424.

Raveendran, P., Fu, J., Wallen, S.L., 2003. Completely green synthesis and stabilization of metal nanoparticles. J. Am. Chem. Soc. 125, 13940–13941.

Sathishkumar, M., Sneha, K., Won, S.W., Cho, C.W., Kim, S., Yun, Y.S., 2009. Cinnamon zeylanicum bark extract and powder mediated green synthesis of nano-crystalline silver particles and its bactericidal activity. Colloids Surf. B Biointerfaces 73, 332–338.

Sau, T., Pal, A., Jana, N.R., Wang, Z.L., Pal, T., 2001. Size controlled synthesis of gold nanoparticles using photochemically prepared seed particles. J. Nanopart. Res. 3, 257–261.

Shankar, S.S., Rai, A., Ahmad, A., Sastry, M., 2004a. Rapid synthesis of Au, Ag, and bimetallic Au core–Ag shell nanoparticles using Neem (Azadirachta indica) leaf broth. J. Colloid Interface Sci. 275, 496–502.

Shankar, S.S., Rai, A., Ankamwar, B., Singh, A., Ahmad, A., Sastry, M., 2004b. Biological synthesis of triangular gold nanoprisms. Nat. Mater. 3, 482–488.

Suman, T.Y., Radhika Rajasree, S.R., Ramkumar, R., Rajthilak, C., Perumal, P., 2014. The green synthesis of gold nanoparticles using an aqueous root extract of Morinda citrifolia L. Spectrochim. Acta Part A 118, 11–16.

Unsworth, L.D., Sheardown, H., Brash, J.L., 2005. Protein resistance of surfaces prepared by sorption of end-thiolated poly(ethylene glycol) to gold: effect of surface chain density. Langmuir 21, 1036–1041.

Vijayakumar, R., Devi, V., Adavallan, K., Saranya, D., 2011. Green synthesis and characterization of gold nanoparticles using extract of anti-tumor potent Crocus sativus. Physica E 44, 665–671.

Xie, J., Zheng, Y., Ying, J.Y., 2009. Protein-directed synthesis of highly fluorescent gold nanoclusters. J. Am. Chem. Soc. 131, 888–889.

Please cite this article in press as: Kanchi, S. et al., Exploitation of de-oiled jatropha waste for gold nanoparticles synthesis: A green approach. Arabian Journal of Chemistry (2014), http://dx.doi.org/10.1016/j.arabjc.2014.08.006